Chemical Geology 593 (2022) 120752

Contents lists available at ScienceDirect

Chemical Geology

journal homepage: www.elsevier.com/locate/chemgeo

Metal recycling tracked by mercury and helium isotopes in platinum–palladium nuggets from Córrego Bom Sucesso, Brazil

Alexandre Raphael Cabral [a,b,*], Changzhou Deng [c], Runsheng Yin [c], Olga V. Yakubovich [d,e], Finlay M. Stuart [f], Miguel Tupinambá [g], Bernd Lehmann [h]

[a] Centro de Pesquisa Professor Manoel Teixeira da Costa, Instituto de Geociências, Universidade Federal de Minas Gerais (UFMG), Belo Horizonte, MG 31270-901, Brazil
[b] Centro de Desenvolvimento da Tecnologia Nuclear (CDTN), Belo Horizonte, MG 31270-901, Brazil
[c] State Key Laboratory of Ore Deposit Geochemistry, Institute of Geochemistry, Chinese Academy of Sciences, Guiyang 550081, China
[d] Saint Petersburg State University, Institute of Earth Sciences, Unversitetskaya emb. 7/9, 199034 Saint-Petersburg, Russia
[e] Institute of Precambrian Geology and Geochronology RAS, Makarova emb. 2, 199034 Saint-Petersburg, Russia
[f] Scottish Universities Environmental Research Centre, Rankine Avenue, East Kilbride G75 0QF, UK
[g] Tektos-Geotectonic Research Group, Faculdade de Geologia, Universidade do Estado do Rio de Janeiro, 20550-050 Rio de Janeiro, RJ, Brazil
[h] Mineral Resources, Technische Universität Clausthal, Adolph-Roemer-Str. 2a, 38678 Clausthal-Zellerfeld, Germany

ARTICLE INFO

Editor: Don Porcelli

Keywords:
Platinum–palladium nuggets
Mercury isotopes
Helium isotopes
Córrego Bom Sucesso
Minas Gerais
Brazil

ABSTRACT

The enigmatic botryoidal nuggets of platinum (Pt) and palladium (Pd) from Córrego Bom Sucesso in the southern Serra do Espinhaço, Minas Gerais, Brazil, are considered to have formed during supergene alteration of placer deposits. This requires hitherto unidentified precious-metal enrichment processes and is inconsistent with Pt–Os age of 180 Ma that entails formation at depth, as recently proposed. Here we report the first mercury (Hg) and helium (He) isotopic determinations of Pt–Pd nuggets. Mercury isotopic compositions have a mass-independent fractionation (MIF) signature with an odd-mass deficit ($\Delta^{199}Hg = -0.22 \pm 0.04$; 1SD, $n = 15$), which requires aqueous photochemical reduction of Hg (II). Extremely low $^{3}He/^{4}He$ (<0.001 R_a) and extremely high concentrations of He (up to 1.9×10^{17} at/g) are indicative of nugget formation from He-enriched fluids within the quartzite sequence of the Espinhaço basin, not from meteoric surface water. The data are consistent with a nugget-forming setting in the deep biosphere, as a result of groundwater interaction with Pt–Pd–Hg minerals in Pan-African-Brasiliano post-orogenic veins. We propose that the negative Hg-MIF signature was inherited from the vein minerals that originally acquired their Hg from Earth's surface during the intracratonic sedimentation of the Proterozoic Espinhaço basin.

1. Introduction

Platinum was sourced from nuggets in placer deposits until the first quarter of the 20th century, prior to the discovery of lode deposits in South Africa and Siberia (e.g., Hattori and Cabri, 1992). Platiniferous placers have their platinum-group minerals as residual grains inherited from magmatic sources (e.g., Kemp, 1902; Hattori and Cabri, 1992; Cabri et al., 1996; Oberthür et al., 2017), apart from a remarkable exception: the placer deposits of Córrego Bom Sucesso, southern Serra do Espinhaço, Minas Gerais, Brazil (Fig. 1). Córrego Bom Sucesso is historically important by providing the nuggets where Pd was first identified (Wollaston, 1809; Hussak, 1906; Cassedanne and Alves, 1992; Cabral et al., 2009). The delicate botryoidal habit and the chemical composition distinguish these nuggets from Pt-rich nuggets of magmatic origin based on the enrichment in Se, Pd and Hg, the virtual absence of Fe and low Ru, Rh, Os and Ir concentrations (Cabral et al., 2019). The botryoidal Pt-rich nuggets of Córrego Bom Sucesso are virtually unique and, as such, cannot be compared to >99% of the world's placer and related deposits of the platinum-group metals (e.g., Cabri et al., 1996). This uniqueness makes them scientifically interesting; a particularity thereof is their enrichment in Hg.

Mercury isotopes are commonly used to reconstruct the geochemical pathways of Hg in modern surface (Blum et al., 2014), as well as in the geological past, from the incorporation of atmospheric Hg into marine

* Corresponding author at: Centro de Pesquisa Professor Manoel Teixeira da Costa, Instituto de Geociências, Universidade Federal de Minas Gerais (UFMG), Belo Horizonte, MG 31270-901, Brazil.
E-mail address: arcab@ufmg.br (A.R. Cabral).

https://doi.org/10.1016/j.chemgeo.2022.120752
Received 13 October 2021; Received in revised form 28 January 2022; Accepted 30 January 2022
Available online 2 February 2022

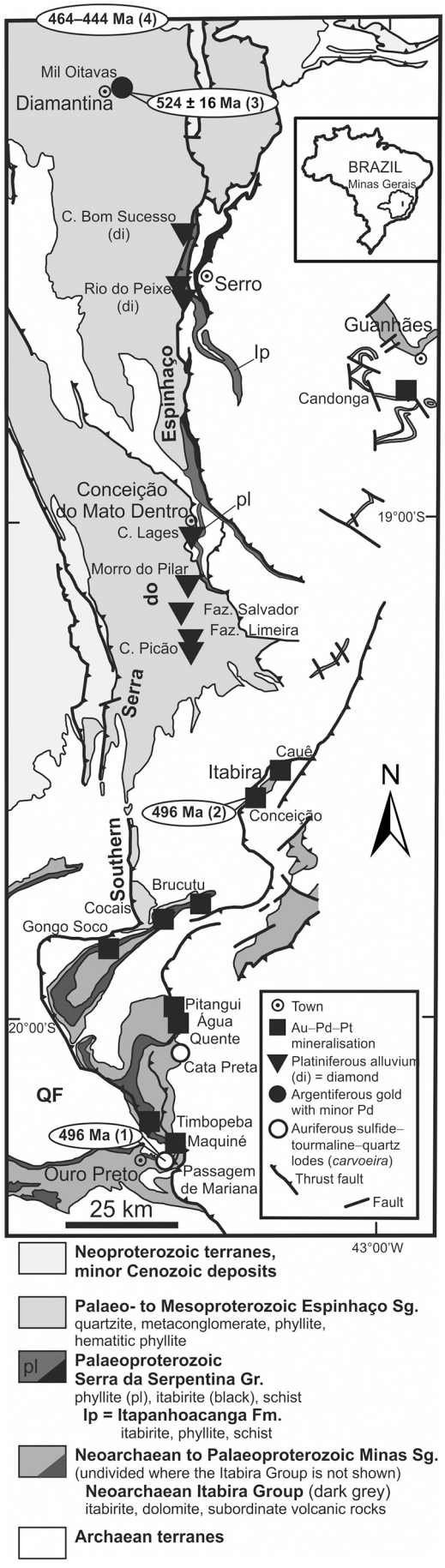

(caption on next column)

Fig. 1. The platiniferous gold–palladium belt of Minas Gerais (Cabral et al., 2009, and references therein). The belt is defined by the distribution of lode and platiniferous placer deposits, which are located along the roughly north–south-trending trace of the Brasiliano thrust faults – i.e., the Araçuaí orogen. Data sources for ages are given in Cabral et al. (2017).
Abbreviations: C. = Córrego (stream); Faz. = Fazenda (farm); Fm. = Formation; Gr. = Group; QF = Quadrilátero Ferrífero; Sg. = Supergroup.

sediments (e.g., Grasby et al., 2020; Shen et al., 2020), through subduction and dehydration, to the formation of Hg-bearing mineral deposits in volcanic arcs (e.g., Deng et al., 2021). This relies on mass-independent-fractionation (MIF) signals that were generated at Earth's surface and survived deep geological processes. Significant MIF of odd-mass-number isotopes of Hg (Δ^{199}Hg and Δ^{201}Hg) is commonly observed at Earth's surface – i.e., in soil/sediment, water, atmosphere and biological samples (Blum et al., 2014). Experiments have demonstrated that the signature results from the photoreduction of Hg(II) and photodegradation of methylmercury in aqueous solutions with dissolved organic matter (Bergquist and Blum, 2007). Other processes, such as evaporation of Hg^0 (Estrade et al., 2009) and dark abiotic reduction of Hg(II) by dissolved organic matter (Zheng and Hintelmann, 2010), can generate MIF of odd-mass Hg isotopes, but the fractionation is too small to explain the Hg-MIF of natural samples (Blum et al., 2014; Blum and Johnson, 2017).

Helium isotopes are a powerful tool for understanding the source of volatiles in hydrothermal minerals (e.g., Stuart et al., 1994). They are particularly suitable for studies of Pt nuggets given the extreme retentivity for He (Shukolyukov et al., 2012a,b). A supergene origin for mineral aggregates requires the precipitation from meteoric solutions which would have a diagnostic isotopic fingerprint, in contrast to the $^3He/^4He$ of crust- and mantle-derived fluids (e.g., Mamyrin and Tolstikhin, 1984). Further, the production of cosmogenic ^{3}He at Earth's surface provides a way to determine the residence time of Pt nuggets in the upper few metres (Yakubovich et al., 2019).

Here we report the Hg and He isotopic compositions of Pt–Pd nuggets from the placer deposit of Córrego Bom Sucesso, for which a biogenic origin has recently been postulated (Cabral et al., 2019; Reith et al., 2019), representing a virtually unique case of authigenic Pt–Pd nuggets at Earth's surface. This view has lately been disputed on the basis of Pt–Os age of ca. 180 Ma and Se isotopes, which suggest nugget formation in the deep biosphere by replacement of hydrothermal vein minerals (Cabral et al., 2021). The Δ^{199}Hg and Δ^{201}Hg signals and reconnaissance He isotopic determinations provide new constraints on the geochemical processes responsible for the generation of the nuggets. Our novel approach implies that precious-metal nuggets can be used as tracers of metal recycling and fluid interaction in the crust.

2. Geological setting and samples

Botryoidal Pt–Pd nuggets were recovered from a heavy-mineral concentrate from Córrego Bom Sucesso, southern Serra do Espinhaço, Minas Gerais, Brazil (Figs. 1, 2). Córrego Bom Sucesso is a stream, with associated placer deposits, in the platiniferous Au–Pd belt of Minas Gerais, approximately 50 km SSE of Diamantina (Fig. 1; Cabral et al., 2009). Platiniferous gravels occur on a bedrock of Mesoproterozoic quartzite in the interstices among quartzite boulders. They consist of quartz sand with subordinate specular hematite, tourmaline, tourmalinite fragments, and minor palladiferous gold, Pt–Pd alloy, hongshiite (PtCu) and potarite (PdHg), among other minerals (Cassedanne et al., 1996; Cabral et al., 2017).

Platinum–osmium age determinations of 5 nuggets are indistinguishable within error at 181 ± 6 Ma (Cabral et al., 2021). The Jurassic age coincides with the final stage of rapid exhumation that brought basement granite-gneissic rocks to ~70 °C (Amaral-Santos et al., 2019). The nugget Pt–Os age also coincides with the emplacement of

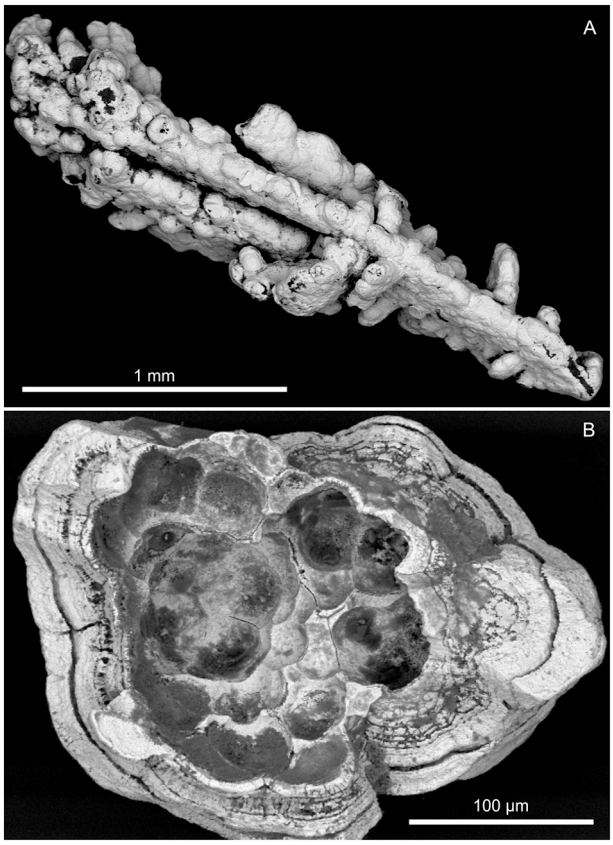

Fig. 2. Backscattered-electron images of Pt–Pd nuggets from Córrego Bom Sucesso. A. Botryoidal, arborescent aggregate. B. Concentric Pt–Pd layers on a hollow core of botryoidal moulds.

Transminas dolerite dykes that occur in the study area (Cabral et al., 2021) and throughout south-eastern Brazil, related to the South Atlantic opening (Chaves and Correia Neves, 2005).

Hematite-bearing quartz veins cross-cut quartzite of the 1.19-Ga Sopa-Brumadinho Formation of the Espinhaço Supergroup (Chemale Jr. et al., 2012) in the Córrego Bom Sucesso catchment. Such veins contain palladiferous gold and a variety of hydrothermal Pt, Pd and Hg minerals, e.g., potarite, hongshiite and jacutingaite (Pt_2HgSe_3) (Cabral et al., 2009, 2017). The veins likely formed after the compressional period of the Brasiliano orogeny (e.g., Cabral et al., 2017), which represents the assembly of West Gondwana (Alkmim et al., 2017, and references therein). Two geodynamic models have been proposed for the formation of Brasiliano orogenic domain in the southern Serra do Espinhaço (the Araçuaí orogen): (i) a subduction–collision model in which subduction of oceanic crust occurred between 630 and 580 Ma (e.g., Alkmim et al., 2017); (ii) an intracontinental (ensialic) model (e.g., Fossen et al., 2020). The Brasiliano orogenic event occurred between 620 and 500 Ma in the southern part of the platiniferous Au–Pd belt (Cabral et al., 2020). Quartz veins, with and without Au–Pd–Pt mineralisation, are late in relation to the main orogenic compression, usually regarded as post-orogenic lodes (e.g., Cabral et al., 2017).

The Pt–Pd nuggets analysed in this study are typically botryoidal and come from the sample set that supplied the nuggets investigated by Cabral et al. (2021). Each sample measured for Hg isotopes represents a whole-nugget analysis ($n = 15$), whereas each nugget selected for He measurements provided a sample aliquot ($n = 5$). The nuggets were recovered by panning from gravels between a rockfall of quartzite boulders and the quartzite bedrock. Consequently, our sampling site differs from that where Reith et al. (2019) obtained their Pt–Pd nuggets.

3. Methods

3.1. Mercury isotopes

Total Hg concentrations (THg) and Hg isotopic compositions were determined at the Institute of Geochemistry, Chinese Academy of Sciences. Fifteen Pt–Pd nuggets of 5–19 mg were digested in a water bath (95 °C) using 5 ml of aqua regia ($HCl:HNO_3 = 3:1$). After digestion, THg was measured in solutions by cold vapour atomic absorption spectrometry (F732-S spectrophotometer, Huaguang Ltd., China). Measurements of reference material, GSS-4 (soil), yielded Hg recoveries of 93 and 113%, and coefficients of variation for triplicate analyses were <9%. The digestion solutions were diluted to 1.0 ng/ml Hg with ~10% acid prior to isotopic analysis using a ThermoFisher Neptune Plus multi-collector inductively coupled plasma mass spectrometer (Yin et al., 2016). Mercury isotopic compositions are reported following convention (Blum and Bergquist, 2007), mass-dependent fractionation expressed in $\delta^{202}Hg$ notation, in per mil, referenced to the NIST-3133 Hg standard analysed before and after each sample:

$$\delta^{202}Hg(‰) = \left[\left(^{202}Hg/^{198}Hg_{sample}\right)/\left(^{202}Hg/^{198}Hg_{standard}\right) - 1\right] \times 1000$$

Mass-independent fractionation is reported in Δ notation, which describes the difference between the measured $\delta^{xxx}Hg$ and the theoretically predicted $\delta^{xxx}Hg$ value, in per mil:

$$\Delta^{xxx}Hg \approx \delta^{xxx}Hg - \delta^{202}Hg \times \beta$$

where β is equal to 0.2520 for ^{199}Hg, 0.5024 for ^{200}Hg, and 0.7520 for ^{201}Hg. The analytical uncertainty is estimated based on replication of the NIST-3177 standard solution, and full procedural analyses of GSS-4. The overall average and uncertainty of NIST-3177 and GSS-4 (Table 1) agree well with previous studies (Blum and Bergquist, 2007; Deng et al., 2021). The higher 2SD uncertainty for either GSS-4 or NIST-3177 is used in calculation of analytical uncertainties.

3.2. Helium isotopes

Temperature-controlled release of ^4He was done at the IPGG RAS on 4 sample aliquots (0.2–6.0 mg), each representing a Pt–Pd nugget. They were weighed and then placed into an ultra-high vacuum chamber for 2 h. All aliquots were stepwise heated and ^4He measured using an MSU-G-01 mass-spectrometric system. Details of the He measurement technique and the design of the instrument are described in Yakubovich et al. (2010). Sensitivity of the mass spectrometer was obtained by repeated measurements of the Knyahinya meteorite standard ($1.24 \pm 0.02\ 10^{-5}$ cm^3 STP/g of ^4He; Schultz and Franke, 2004). The complete procedural blank determined by heating the empty Re cuvette to 1450 °C was 1.3×10^9 atoms. The aliquots of Pt–Pd nuggets were heated up to 1400 °C in a series of steps, from 3 to 17, the total heating time of which was between 60 and 80 min. Being the MSU-G-01-M system a low-resolution mass spectrometer, $^3He/^4He$ ratios were not measured.

Helium isotopic composition was determined in one aliquot from another Pt–Pd nugget in a modified ThermoFisher Helix-SFT mass spectrometer at the SUERC (Carracedo et al., 2019). Sensitivity and mass fractionation were obtained by repeated measurements of aliquots of He from a tank of the HESJ standard (Matsuda et al., 2002). A Pt foil was melted in order to determine a representative hot blank level to correct the He concentrations released by heating the sample aliquot. The averages of ^3He and ^4He blanks were 1.5×10^4 atoms and 7×10^8 atoms, respectively. Helium was extracted by directly heating the sample aliquot with a focused beam of an 808-nm diode laser (Stuart et al., 1999), following the protocol described in Yakubovich et al. (2019).

The decay of ^{238}U, ^{235}U and ^{232}Th in Pt minerals generates ^4He in addition to the decay of ^{190}Pt (Shukolyukov et al., 2012b). The aliquot of Pt–Pd nugget degassed at the SUERC was dissolved in aqua regia at 130 °C for 24 h. Uranium and Th concentrations were measured in 5% HNO_3

Table 1
Results of measurements for Hg isotopes in Pt–Pd nuggets from Córrego Bom Sucesso, Minas Gerais, and in reference materials.

	Hg*	δ^{199}Hg	δ^{200}Hg	δ^{201}Hg	δ^{202}Hg	Δ^{199}Hg	Δ^{200}Hg	Δ^{201}Hg
Nugget	(%)	(‰)	(‰)	(‰)	(‰)	(‰)	(‰)	(‰)
1	2.73	−0.19	0.15	0.11	0.39	−0.29	−0.05	−0.18
2	4.35	−0.15	0.35	0.25	0.50	−0.27	0.10	−0.12
3	2.10	−0.19	−0.01	−0.23	0.01	−0.20	−0.01	−0.24
4	8.33	−0.14	0.05	−0.03	0.22	−0.19	−0.06	−0.19
5	1.05	−0.21	0.01	−0.18	0.08	−0.23	−0.03	−0.24
6	3.57	−0.13	0.21	0.11	0.52	−0.27	−0.06	−0.28
7	6.40	−0.22	0.05	−0.14	0.16	−0.26	−0.02	−0.26
8	3.12	−0.28	−0.07	−0.29	−0.14	−0.24	0.00	−0.19
9	7.37	−0.09	0.11	0.12	0.32	−0.16	−0.05	−0.12
10	1.45	−0.14	0.08	−0.07	0.12	−0.17	0.01	−0.16
11	3.63	−0.27	−0.08	−0.29	−0.17	−0.23	0.00	−0.16
12	5.91	−0.09	0.08	−0.04	0.21	−0.15	−0.03	−0.20
13	2.63	−0.27	−0.14	−0.35	−0.25	−0.21	−0.02	−0.17
14	4.91	−0.23	0.10	−0.19	0.07	−0.25	0.06	−0.24
15	1.88	−0.10	0.21	0.18	0.49	−0.22	−0.03	−0.18
Reference material								
	(ng/g)							
GSS-4	590	−0.88	−0.89	−1.72	−1.79	−0.43	0.01	−0.38
GSS-4	590	−0.86	−0.87	−1.74	−1.74	−0.42	0.00	−0.43
GSS-4	590	−0.82	−0.86	−1.76	−1.77	−0.38	0.03	−0.43
Mean		−0.85	−0.87	−1.74	−1.76	−0.41	0.01	−0.41
2SD		0.06	0.04	0.03	0.05	0.06	0.03	0.06
	(ng/ml)							
NIST3177	1	−0.10	−0.24	−0.44	−0.51	0.03	0.02	−0.05
NIST 3177	1	−0.16	−0.25	−0.46	−0.53	−0.03	0.01	−0.06
NIST 3177	1	−0.16	−0.31	−0.43	−0.55	−0.02	−0.03	−0.02
Mean		−0.14	−0.27	−0.44	−0.53	−0.01	0.00	−0.05
2SD		0.06	0.07	0.03	0.04	0.06	0.05	0.04

* Total Hg.

(1.5 ml) solution employing a ThermoFisher ELEMENT XR ICP–MS (GEOKHI RAS). The instrument was set for medium resolution, which removed interference from $^{40}Ar^{195}Pt^{+}$ and $^{40}Ar^{198}Pt^{+}$ ions. Fresh mono-elemental solutions of U and Th (Inorganic Ventures) were used for calibrating the mass spectrometer. The full chemistry blank did not exceed 0.7 ng/kg both for ^{238}U and ^{232}Th.

4. Results

4.1. Mercury isotopes

Total Hg concentrations and Hg isotopic ratios for Pt–Pd nuggets from Córrego Bom Sucesso are presented in Table 1. Each value refers to a whole-nugget analysis. Value ranges are as follows: $1.05 \leq THg \leq 8.33\%$; $-0.28 \leq \delta^{199}Hg \leq -0.09‰$; $-0.14 \leq \delta^{200}Hg \leq +0.35‰$; $-0.35 \leq \delta^{201}Hg \leq +0.25‰$; $-0.25 \leq \delta^{202}Hg \leq +0.52‰$. The ranges show consistently

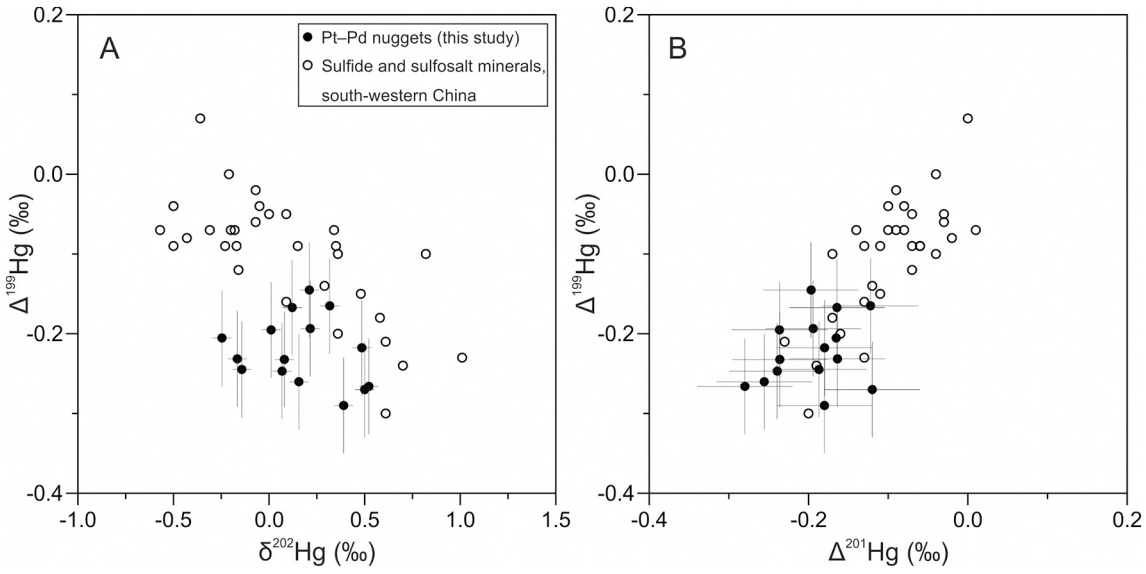

Fig. 3. Plots of $\delta^{202}Hg$ vs. $\Delta^{199}Hg$ (A) and $\Delta^{201}Hg$ vs. $\Delta^{199}Hg$ (B) for the Bom Sucesso Pt–Pd nuggets. For comparison, sulfide and sulfosalt minerals from sediment-hosted lead–zinc deposits in south-western China are also plotted (Xu et al., 2018). Those hydrothermal minerals likely incorporated the Hg-isotope MIF from the metamorphic country rocks, which preserved surface MIF signals from terrestrial environments (negative odd-MIF values). Crosses refer to analytical uncertainties – i.e., 2SD values in reference materials, Table 1).

negative odd-MIF signals, with Δ^{199}Hg and Δ^{201}Hg between −0.29 and −0.15‰, and between −0.28 and −0.12‰, respectively. For comparison, plots of δ^{202}Hg vs. Δ^{199}Hg (Fig. 3A) and Δ^{201}Hg vs. Δ^{199}Hg (Fig. 3B) for the Bom Sucesso Pt–Pd nuggets are shown together with data for sulfide and sulfosalt minerals from sediment-hosted Pb–Zn deposits in southwestern China (Xu et al., 2018). Those minerals display trends that marginally overlap with the Pt–Pd nuggets, which have a more restricted distribution without any trend (Fig. 3).

4.2. Helium isotopes

Helium concentrations in the Pt–Pd nuggets vary by nearly an order of magnitude, from 3 to 19 × 10^{16} at/g (Table 2). In both laboratories, the ^{4}He hot blank level is less than 0.1% of that released from the nuggets. Total contribution of ^{3}He from the blank was less than 10%. One nugget aliquot has a ^{3}He/^{4}He ratio of 1.9 ± 0.8 × 10^{-9} (0.0014 ± $\frac{0.003}{0.0013}$ R_a, using the standard air normalisation), which is indicative of a purely radiogenic He (Mamyrin and Tolstikhin, 1984; Ballentine and Burnard, 2002). The low ^{3}He/^{4}He rules out significant contribution of magmatic He (e.g., Stuart et al., 1994), or identification of cosmogenic ^{3}He that would imply exposure at Earth's surface (e.g., Yakubovich et al., 2019).

The low-^{3}He/^{4}He nugget has U and Th contents that are below the detection limit, corresponding to less than 45 ng/g U and 25 ng/g Th. If all the nugget ^{4}He originated from the in situ decay of ^{190}Pt, the nuggets would have unrealistic Pt–He ages (60–340 Ga). Assuming a ^{190}Pt–^{186}Os age of 181 Ma (Cabral et al., 2021), less than 2% of the ^{4}He released from the Pt–Pd nuggets could be derived from in situ radiogenic decay of U and Th, implying that the nugget-trapped He comes from an external source. The ^{4}He release occurred above 1000 °C, typically in the temperature range of 1200–1400 °C, as several distinct peaks (Fig. 4). This is different from a typical release of in situ radiogenic He from native metals, characterised by a "burst-like" He release at temperatures close to the melting point of the metal (Shukolyukov et al., 2012a,b), supporting an origin for the He in a trapped fluid phase – i.e., fluid inclusions in the nugget Pt–Pd matrix.

5. Discussion

5.1. Constraints on the origin of the Bom Sucesso Pt–Pd nuggets from Hg isotopes

A local magmatic source of Pt and Pd has been advanced by Cassedanne et al. (1996) and Fleet et al. (2002). For example, Fleet et al. (2002) argue that Pt and Pd would have been remobilised by "high-level episodic hydrothermal alteration of mafic and ultramafic rocks within the drainage basin", with the precipitation of Pt–Pd nuggets as open-space fillings in the country-rock quartzite. A magmatic metal source could be traced by Hg isotopes. Negligible Hg-MIF signals – i.e., Δ^{199}Hg and Δ^{201}Hg of ~0‰ – have been observed in hydrothermal fluids from the Guaymas Basin sea-floor rift (Sherman et al., 2009). The

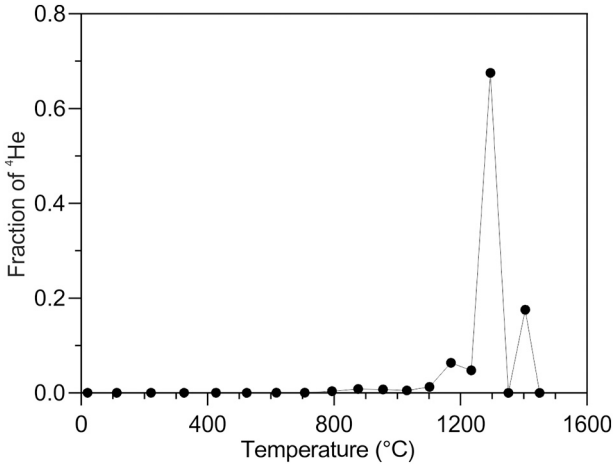

Fig. 4. Kinetics of thermodesorption of ^{4}He from an aliquot of Pt–Pd nugget (0.183 mg). Duration of each step of heating was 280 s. Step-heating measurements are presented in Supplementary Table S1 (Electronic Supplementary Material).

significantly negative Δ^{199}Hg and Δ^{201}Hg signals of our samples (Table 1) rule out a mantle source for the Hg, either directly transferred from a silicate magma or leached from mafic rocks. By extension, the nugget-forming precious metals Pt and Pd are unlikely to have been sourced from a mantle-derived magma, such as Mesozoic dolerite intrusions in the Espinhaco Supergroup. The most likely source for Pt, Pd and Hg are hydrothermal minerals, such as potarite, hongshiite and jacutingaite, formed in the hematite-bearing quartz veins that characterise the platiniferous Au–Pd belt of Minas Gerais (e.g., Cabral et al., 2009, 2017). Mercury occurs as a minor component in hongshiite, whereas it is a major element in potarite and jacutingaite (Cabral et al., 2008).

Further constraints can be placed on the Bom Sucesso Pt–Pd nuggets by the Δ^{199}Hg/Δ^{201}Hg ratio, which has been used to identify pathways of Hg isotopic fractionation (e.g., Blum et al., 2014). For example, sulfide and sulfosalt minerals from hydrothermal deposits display Δ^{199}Hg/Δ^{201}Hg ~ 1.0 (Xu et al., 2018; Deng et al., 2021), which is close to that reported from experimental photoreduction of aqueous Hg(II) (Bergquist and Blum, 2007). The Pt–Pd nuggets have odd-MIF signals that are distributed along the line defined by Δ^{199}Hg/Δ^{201}Hg = 1.0 (Fig. 3B), suggesting that the MIF was driven by aqueous Hg(II) photoreduction. On the other hand, the Pt–Pd nuggets appear to have been formed by microbial mediation (Reith et al., 2019; Cabral et al., 2021). Microbial reduction of aqueous Hg(II) has experimentally induced mass-dependent fractionation only, leading to isotopically lighter Hg(0) (Kritee et al., 2007). The data dispersion in Fig. 3A likely reflects nugget-forming microbial reduction of aqueous Hg(II) with odd-MIF signals, mostly from photochemical reduction.

The negative odd-MIF signal of photochemical reduction requires

Table 2
Results of measurements for He isotopes in Pt–Pd nuggets from Córrego Bom Sucesso, Minas Gerais.

Nugget	Mass (mg)	^{4}He (10^{10} at)	1SD	^{3}He (10^4 at)	1SD	R/Ra	^{4}He (10^{16} at/g)	1SD
1*	2.272	8700	500	16.0	6.7	0.0014	3.8	0.2
2	0.183	3400	220	–	–	–	18.6	1.3
3	6.05	43,500	130	–	–	–	7.2	0.02
4	0.21	2550	30	–	–	–	12.1	0.33
5	0.28	700	17	–	–	–	2.5	0.07
Hot blank								
SUERC		0.07	0.03	1.50	1.10	17	–	–
IPGG RAS		0.13	0.8	–	–	–	–	–

* Measurement performed at the SUERC; all others at the IPGG RAS.

that the Hg in the Pt–Pd nuggets was exposed to sunlight. Two pathways are possible: (i) supergene solutions carried Hg from the surface to the site of nugget formation within the placer deposit; or (ii) Hg-bearing hydrothermal minerals with the odd-MIF signal were dissolved to release Hg and also Pt and Pd to form nuggets at depth.

5.2. Constraints on the origin of the Bom Sucesso Pt–Pd nuggets from He data

The He isotopic composition of the trapped fluid can be used as a tracer of the environment of Pt–Pd nugget formation. The reconnaissance He isotopic data rule out the possibility of Pt–Pd nugget formation within the placer deposit in equilibrium with surface fluids. Firstly, the low atmospheric He concentration means that, if the He were derived from air-equilibrated aqueous fluids, the nuggets would require the incorporation of ~3 g of water into 2.3-mg nugget. Secondly, although only one $^{3}He/^{4}He$ ratio has been determined, the value (0.0014 R_a) is three orders of magnitude lower than the atmospheric ratio.

Our reconnaissance data indicate that the Pt–Pd nuggets were generated in the presence of He-rich crustal fluids. Hydrothermal fluids associated with magmatism typically show $^{3}He/^{4}He$ ratios in range of 0.1–5 R_a (Stuart et al., 1994, 1995; Burnard and Polya, 2003; Graupner et al., 2006; Jin et al., 2020). Low $^{3}He/^{4}He$ ratios are typical of aquifers in Li-poor (<15 μg/g Li) crustal rocks (e.g., Castro, 2004; Ballentine and Burnard, 2002). The He isotopic data are compatible with Pt–Pd nuggets having interacted with old fluids that had previously equilibrated with old Li-poor bedrock. Possible source rocks include the quartzite-dominated metasedimentary sequence of the southern Serra do Espinhaço. In the cratonic region west of the southern Serra do Espinhaço, faults that cut the Archaean and Palaeoproterozoic basement and supracrustal rocks are thought to drain deep-seated hydrogen (Donzé et al., 2020), possibly of radiolysis origin, and He with a diagnostic crustal signature (<0.02 Ra; Flude et al., 2019).

Hydrothermal fluids trapped in minerals usually do not exceed 10^{-6} cm^3 STP He/g (e.g., Stuart et al., 1994, 1995; Burnard and Polya, 2003; Graupner et al., 2006; Jin et al., 2020). If we assume that Pt–Pd alloys trapped fluids in the same way as other hydrothermal minerals, the fluids would be 2–3 orders of magnitude richer in He. Heating of ancient crust induces He degassing from minerals, resulting in the formation of He-rich groundwaters. Alternatively, He-rich groundwaters might be produced due to the long-term interaction between the water and a source rock. Given that the time of nugget formation is coeval with the South Atlantic opening (e.g., Chaves and Correia Neves, 2005), both scenarios are possible.

The depth at which the Pt–Pd nuggets formed can be estimated from the mean denudation rate, determined by cosmogenic ^{10}Be produced in alluvial sediments on the quartzite substratum of the Diamantina region. The mean denudation rate of 4.4 m/m.y. (Barreto et al., 2013), combined with the nugget Pt–Os age (181 Ma), suggests that they formed at approximately 800 m below the surface (Cabral et al., 2021). This is in line with thermochronological modeling using apatite-fission-track (AFT) data from basement granitic-gneissic rocks (Amaral-Santos et al., 2019). The AFT thermal modeling indicates that the temperature at about 800 m below the surface 180 m.y. ago was approximately 70 °C. It is likely that at this depth the groundwater reached quartzite-hosted hydrothermal veins with high concentrations of Pt–Pd–Hg-bearing minerals, having replaced them in situ. The replacement would have involved removal of more soluble metals, such as As, Sb and Se, and relative enrichment of Pt, Pd and Hg. Alternatively, the groundwater could have obtained its metal load from the dissolution of Pt–Pd–Hg-bearing minerals in nearby hematite–quartz veins. In both scenarios, the estimated groundwater depth is within the conditions under which microbial life would have existed to account for the presence of iodine and organic matter remains in the Bom Sucesso Pt–Pd nuggets, and their Se isotopic values (Cabral et al., 2021).

5.3. Mercury recycling and geotectonic implication

These new constraints on the origin of the Bom Sucesso Pt–Pd nuggets indicate that the Hg isotopic signature was inherited from earlier vein minerals that contained recycled Hg from the continental crust. The negative $\Delta^{199}Hg$ values for the Pt–Pd nuggets are typical of terrestrial Hg (Blum et al., 2014; Grasby et al., 2017; Shen et al., 2019; Them II et al., 2019). Photoreduction of Hg(II) generates negative $\Delta^{199}Hg$ in the product gaseous Hg(0), and positive $\Delta^{199}Hg$ in the residual Hg(II) phase (Bergquist and Blum, 2007). For this reason, terrestrial pools – e.g., soil and vegetation – mainly show negative $\Delta^{199}Hg$ due to the primary accumulation of Hg(0), whereas ocean pools – e.g., marine sediments and seawater – mainly show positive $\Delta^{199}Hg$ because of wet deposition of Hg(II) (Blum et al., 2014). The characteristic $\Delta^{199}Hg$ of seawater-mediated Hg deposition can be used to track subduction-related volcanic inputs (Shen et al., 2021). Once acquired in surface reservoirs, MIF signals of Hg isotopes remain even after Hg recycling through subduction zones to form volcanic-arc-related, Hg-bearing epithermal deposits, where inherited positive $\Delta^{199}Hg$ values of marine sediments and seawater have been found (Deng et al., 2021).

As the seawater $\Delta^{199}Hg$ signal is missing in the Pt–Pd nuggets, it seems that Hg was recycled into the hematite–quartz veins from continental sedimentary material. Because the veins are late in relation to the Araçuaí orogen, they likely captured post-orogenic fluids from continental sedimentary rocks. It is interesting to note that the Pt–Pd minerals of hematite–quartz veins have a Hg–As–Sb metal association that is characteristic of low-temperature hydrothermal deposits in a continental setting, such as the Au and Sb deposits of South China with negative Hg-MIF signals (Yin et al., 2019; Fu et al., 2020; the maximum contents of total Hg reported therein are 111 and 97 μg/g, respectively). If continental sedimentary rocks provided metals for late-orogenic fluids, the veins that resulted from them would have carried $\Delta^{199}Hg$ signals of terrestrial surface reservoirs. Mercury recycling and its isotopic signal from a terrestrial surface setting can be exemplified by river systems in California, the suspended particulate matter of which retains the product of Hg photoreduction within fluvial surface waters, leading to characteristically negative $\Delta^{199}Hg$ values in the particulate fraction (Washburn et al., 2019). Our Hg isotopic data support an ensialic setting for Hg cycling, without any traceable contribution of Hg from marine sediments or hydrated oceanic crust, the positive seawater $\Delta^{199}Hg$ signal of which can be retrieved from epithermal veins (Deng et al., 2021).

6. Conclusion

The Bom Sucesso Pt–Pd nuggets are widely cited as an example of supergene accumulation of precious metals within alluvial sediments, but this model cannot explain the new Hg and He isotopic data presented here, which indicate that the nuggets formed in the subsurface, in an environment dominated by ancient groundwater. The nuggets are an example of precious-metal recycling, which is tracked by the odd-MIF signal of Hg isotopes, captured at Earth's surface and kept through diagenesis, metamorphism, orogenesis and fluid overprint.

Supplementary data to this article can be found online at https://doi.org/10.1016/j.chemgeo.2022.120752.

Declaration of Competing Interest

The authors declare that they have no known competing financial interests or personal relationships that could have appeared to influence the work reported in this paper.

Acknowledgements

The research centre Physical Methods of Surface Investigation, Saint-Petersburg State University, is acknowledged for assistance in

measurements of He thermodesorption from Pt–Pd alloys. Luigia Di Nicola's assistance at the SUERC noble gas laboratory is also appreciated. Rogerio Kwitko-Ribeiro is thanked for generating the BSE images of Fig. 2. This research was supported by the SUERC, State Task of the IPGG RAS (FMNU-2022-0003). An anonymous colleague, Louis J. Cabri and Andy Hunt are gratefully acknowledged for their thoughtful reviews, which have considerably improved the manuscript, as well as Donald Porcelli for his diligent editorial handling.

References

Alkmim, F.F., Kuchenbecker, M., Reis, H.L.S., Pedrosa-Soares, A.C., 2017. The Araçuaí belt. In: Heilbron, M., Cordani, U., Alkmim, F. (Eds.), São Francisco Craton, Eastern Brazil. Regional Geology Reviews. Springer, Cham. https://doi.org/10.1007/978-3-319-01715-0_14.

Amaral-Santos, E., Jelinek, A.R., Almeida-Abreu, P.A., Genezine, F.A., 2019. Phanerozoic cooling history of Archean/Paleoproterozoic basement in the southern Espinhaço Range, southeastern Brazil, through apatite fission-track analysis. J. S. Am. Earth Sci. 96, 102352.

Ballentine, C.J., Burnard, P.G., 2002. Production, release and transport of noble gases in the continental crust. Rev. Mineral. Geochem. 47, 481–538.

Barreto, H.N., Varajão, C.A.C., Braucher, R., Bourlès, D.L., Salgado, A.A.R., Varajão, A.F. D.C., 2013. Denudation rates of the Southern Espinhaço Range, Minas Gerais, Brazil, determined by in situ-produced cosmogenic beryllium-10. Geomorphology 191, 1–13.

Bergquist, B.A., Blum, J.D., 2007. Mass-dependent and -independent fractionation of Hg isotopes by photoreduction in aquatic systems. Science 318, 417–420.

Blum, J.D., Bergquist, B.A., 2007. Reporting of variations in the natural isotopic composition of mercury. Anal. Bioanal. Chem. 388, 353–359.

Blum, J.D., Johnson, M.W., 2017. Recent developments in mercury stable isotope analysis. Rev. Mineral. Geochem. 82, 733–757.

Blum, J.D., Sherman, L.S., Johnson, M.W., 2014. Mercury isotopes in earth and environmental sciences. Annu. Rev. Earth Planet. Sci. 42, 249–269.

Burnard, P.G., Polya, D.A., 2003. Importance of mantle derived fluids during granite associated hydrothermal circulation: He and Ar isotopes of ore minerals from Panasqueira. Geochim. Cosmochim. Acta 68, 1607–1615.

Cabral, A.R., Galbiatti, H.F., Kwitko-Ribeiro, R., Lehmann, B., 2008. Platinum enrichment at low temperatures and related microstructures, with examples of hongshiite (PtCu) and empirical 'Pt_2HgSe_3' from Itabira, Minas Gerais, Brazil. Terra Nova 20, 32–37.

Cabral, A.R., Lehmann, B., Tupinambá, M., Schlosser, S., Kwitko-Ribeiro, R., de Abreu, F. R., 2009. The platiniferous Au–Pd belt of Minas Gerais, Brazil, and genesis of its botryoidal Pt–Pd–Hg aggregates. Econ. Geol. 104, 1265–1276.

Cabral, A.R., Tupinambá, M., Zeh, A., Lehmann, B., Wiedenbeck, M., Brauns, M., Kwitko-Ribeiro, R., 2017. Platiniferous gold–tourmaline aggregates in the gold–palladium belt of Minas Gerais, Brazil: implications for regional boron metasomatism. Mineral. Petrol. 111, 807–819.

Cabral, A.R., Zack, T., König, S., Eickmann, B., Kwitko-Ribeiro, R., Tupinambá, M., Lehmann, B., 2019. Distinguishing high- from low-temperature platinum nuggets through their trace-element pattern. Econ. Geol. 114, 201–206.

Cabral, A.R., Zeh, A., Tupinambá, M., Pimenta, J., 2020. First evidence for Neoproterozoic magmatism in the Quadrilátero Ferrífero of Minas Gerais, Brazil, and geotectonic implications. J. S. Am. Earth Sci. 104, 102844.

Cabral, A.R., König, S., Eickmann, B., Brauns, M., Tupinambá, M., Lehmann, B., Varas-Reus, M.I., 2021. Extreme fractionation of selenium isotopes and possible deep biospheric origin of platinum nuggets from Minas Gerais, Brazil. Geology 49, 1327–1331. https://doi.org/10.1130/G49088.1.

Cabri, L.J., Harris, D.C., Weiser, T.W., 1996. Mineralogy and distribution of platinum-group mineral (PGM) placer deposits of the world. Explor. Min. Geol. 5, 73–167.

Carracedo, A., Rodés, Á., Smellie, J., Stuart, F.M., 2019. Episodic erosion in West Antarctica inferred from cosmogenic ^{3}He and ^{10}Be in olivine from Mount Hampton. Geomorphology 327, 438–445.

Cassedanne, J.P., Alves, J.N., 1992. Palladium and platinum from Córrego Bom Sucesso, Minas Gerais, Brazil. Mineral. Rec. 23, 471–474.

Cassedanne, J.P., Jedwab, J., Alves, J.N., 1996. Apport d'une prospection systématique à l'étude de l'origine de l'or et du platine alluviaux du Córrego Bom Sucesso (Serro – Minas Gerais). An. Acad. Bras. Ciê. 68, 569–582.

Castro, M.C., 2004. Helium sources in passive margin aquifers—new evidence for a significant mantle ^{3}He source in aquifers with unexpectedly low in situ ^{3}He/^{4}He production. Earth Planet. Sci. Lett. 222, 897–913.

Chaves, A.O., Correia Neves, J.M., 2005. Radiometric ages, aeromagnetic expression, and general geology of mafic dykes from southeastern Brazil and implications for African–South American correlations. J. S. Am. Earth Sci. 19, 387–397.

Chemale Jr., F., Dussin, I.A., Alkmim, F.F., Martins, M.S., Queiroga, G., Armstrong, R., Santos, M.N., 2012. Unravelling a Proterozoic basin history through detrital zircon geochronology: the case of the Espinhaço Supergroup, Minas Gerais, Brazil. Gondwana Res. 22, 200–206.

Deng, C., Sun, G., Rong, Y., Sun, R., Sun, D., Lehmann, B., Yin, R., 2021. Recycling of mercury from the atmosphere-ocean system into volcanic-arc–associated epithermal gold systems. Geology 49, 309–313.

Donzé, F.-V., Truche, L., Namin, P.S., Lefeuvre, N., Bazarkina, E.F., 2020. Migration of natural hydrogen from deep-seated sources in the São Francisco basin, Brazil. Geosciences 10, 346.

Estrade, N., Carignan, J., Sonke, J.E., Donard, O.F.X., 2009. Mercury isotope fractionation during liquid–vapor evaporation experiments. Geochim. Cosmochim. Acta 73, 2693–2711.

Fleet, M.E., de Almeida, C.M., Angeli, N., 2002. Botryoidal platinum, palladium and potarite from the Bom Sucesso stream, Minas Gerais, Brazil: compositional zoning and origin. Can. Mineral. 40, 341–355.

Flude, S., Warr, O., Magalhães, N., Bordmann, V., Fleury, J.M., Reis, H.L.S., Trindade, R. I., Hillegonds, D., Sherwood Lollar, B., Ballentine, C.J., 2019. Deep crustal source for hydrogen and helium gases in the São Francisco Basin, Minas Gerais, Brazil. In: AGUFM 2019. EP51D-2111.

Fossen, H., Cavalcante, C., Konopásek, J., Meira, V.T., de Almeida, R.P., Hollanda, M.H. B.M., Trompette, R., 2020. A critical discussion of the subduction-collision model for the Neoproterozoic Araçuaí-West Congo orogen. Precambrian Res. 343, 105715.

Fu, S., Hu, R., Yin, R., Yan, J., Mi, X., Song, Z., Sullivan, N.A., 2020. Mercury and in situ sulfur isotopes as constraints on the metal and sulfur sources for the world's largest Sb deposit at Xikuangshan, southern China. Mineral. Deposita 55, 1353–1364.

Grasby, S.E., Shen, W., Yin, R., Gleason, J.D., Blum, J.D., Lepak, R.F., Hurley, J.P., Beauchamp, B., 2017. Isotopic signatures of mercury contamination in latest Permian oceans. Geology 45, 55–58.

Grasby, S.E., Them II, T.R., Chen, Z., Yin, R., Ardakani, O.H., 2020. Mercury as a proxy for volcanic emissions in the geologic record. Earth-Sci. Rev. 196, 102880.

Graupner, T., Niedermann, S., Kempe, U., Klemd, R., Bechtel, A., 2006. Origin of ore fluids in the Muruntau gold system: Constraints from noble gas, carbon isotope and halogen data. Geochim. Cosmochim. Acta 70, 5356–5370.

Hattori, K., Cabri, L.J., 1992. Origin of platinum-group-mineral nuggets inferred from an osmium-isotope study. Can. Mineral. 30, 289–301.

Hussak, E., 1906. Über das Vorkommen von Palladium und Platin in Brasilien. Z. Prakt. Geol. 14, 284–293.

Jin, X.Y., Hofstra, A.H., Hunt, A.G., Liu, J.Z., Yang, W., Li, J.W., 2020. Noble gases fingerprint the source and evolution of ore-forming fluids of Carlin-type gold deposits in the Golden Triangle, South China. Econ. Geol. 115, 455–459.

Kemp, J.F., 1902. The geological relations and distribution of platinum and associated metals. Bull. U. S. Geol. Surv. 193 https://doi.org/10.3133/b193.

Kritee, K., Blum, J.D., Johnson, M.W., Bergquist, B.A., Barkay, T., 2007. Mercury stable isotope fractionation during reduction of Hg (II) to Hg (0) by mercury resistant microorganisms. Environ. Sci. Technol. 41, 1889–1895.

Mamyrin, B.A., Tolstikhin, I.N., 1984. Helium Isotopes in Nature. Elsevier, Amsterdam, p. 274.

Matsuda, J.M., Matsumoto, T.M., Sumino, H.S., Nagao, K.N., Yamamoto, J.Y., Miura, Y. M., Kaneoka, I.K., Takahata, N.T., Sano, Y.S., 2002. The ^{3}He/^{4}He ratio of the new internal He standard of Japan (HESJ). Geochem. J. 36, 191–195.

Oberthür, T., Melcher, F., Weiser, T.W., 2017. Detrital platinum-group minerals and gold in placers of southeastern Samar Island, Philippines. Can. Mineral. 55, 45–62.

Reith, F., Nolze, G., Saliwan-Neumann, R., Etschmann, B., Kilburn, M.R., Brugger, J., 2019. Unraveling the formation histories of placer gold and platinum-group mineral particles from Córrego Bom Sucesso, Brazil: a window into noble metal cycling. Gondwana Res. 76, 246–259.

Schultz, L., Franke, L., 2004. Helium, neon, and argon in meteorites: a data collection. Meteorit. Planet. Sci. 39, 1889–1890.

Shen, J., Yu, J., Chen, J., Algeo, T.J., Xu, G., Feng, Q., Shi, X., Planavsky, N.J., Shu, W., Xie, S., 2019. Mercury evidence of intense volcanic effects on land during the Permian–Triassic transition. Geology 47, 1117–1121.

Shen, J., Feng, Q., Algeo, T.J., Liu, J., Zhou, C., Wei, W., Liu, J., Them II, T.R., Gill, B.C., Chen, J., 2020. Sedimentary host phases of mercury (Hg) and implications for use of Hg as a volcanic proxy. Earth Planet. Sci. Lett. 543, 116333.

Shen, J., Chen, J., Algeo, T.J., Feng, Q., Yu, J., Xu, Y.-G., Xu, G., Lei, Y., Planavsky, N.J., Shucheng Xie, S., 2021. Mercury fluxes record regional volcanism in the South China craton prior to the end-Permian mass extinction. Geology 49, 452–456.

Sherman, L.S., Blum, J.D., Nordstrom, D.K., McCleskey, R.B., Barkay, T., Vetriani, C., 2009. Mercury isotopic composition of hydrothermal systems in the Yellowstone Plateau volcanic field and Guaymas Basin sea-floor rift. Earth Planet. Sci. Lett. 279, 86–96.

Shukolyukov, Y.A., Yakubovich, O.V., Yakovleva, S.Z., Sal'nikova, E.B., Kotov, A.B., Rytsk, E.Y., 2012a. Geothermochronology based on noble gases: III. Migration of radiogenic He in the crystal structure of native metals with applications to their isotopic dating. Petrol 20, 1–20.

Shukolyukov, Y.A., Yakubovich, O.V., Mochalov, A.G., Kotov, A.B., Sal'nikova, E.B., Yakovleva, S.Z., Korneev, S.I., Gorokhovskii, B.M., 2012b. New geochronometer for the direct isotopic dating of native platinum minerals (^{190}Pt–^{4}He method). Petrol 20, 491–505.

Stuart, F.M., Turner, G., Duckworth, R.C., Fallick, A.E., 1994. Helium isotopes as tracers of trapped hydrothermal fluids in ocean-floor sulfides. Geology 22, 823–826.

Stuart, F.M., Burnard, P., Taylor, R., Turner, G., 1995. Resolving mantle and crustal contributions to ancient hydrothermal fluids: He–Ar isotopes in fluid inclusions from Dae Hwa W–Mo mineralisation, South Korea. Geochim. Cosmochim. Acta 59, 4663–4673.

Stuart, F.M., Harrop, P.J., Knott, S., Turner, G., 1999. Laser extraction of helium isotopes from Antarctic micrometeorites: source of He and implications for the flux of extraterrestrial ^{3}He to Earth. Geochim. Cosmochim. Acta 93, 2653–2665.

Them II, T.R., Jagoe, C.H., Caruthers, A.H., Gill, B.C., Grasby, S.E., Gröcke, D.R., Yin, R., Owens, J.D., 2019. Terrestrial sources as the primary delivery mechanism of mercury to the oceans across the Toarcian Oceanic Anoxic Event (Early Jurassic). Earth Planet. Sci. Lett. 507, 62–72.

Washburn, S.J., Blum, J.D., Donovan, P.M., Singer, M.B., 2019. Isotopic evidence for mercury photoreduction and retention on particles in surface waters of Central California, USA. Sci. Total Environ. 674, 451–461.

Wollaston, W.H., 1809. On platina and native palladium from Brasil. Phil. Trans. R. Soc. A 99, 189–194.
Xu, C., Yin, R., Peng, J., Hurley, J.P., Lepak, R.F., Gao, J., Feng, X., Hu, R., Bi, X., 2018. Mercury isotope constraints on the source for sediment-hosted lead–zinc deposits in the Changdu area, southwestern China. Mineral. Deposita 53, 339–352.
Yakubovich, O.V., Shukolyukov, Y.A., Kotov, A.B., Yakovleva, S.Z., Sal'nikova, E.B., 2010. Geothermochronology based on noble gases: II. Stability of the (U–Th)/He isotope system in zircon. Petrol 18, 579–594.
Yakubovich, O.V., Stuart, F.M., Nesterenok, A.V., Carracedo, A., 2019. Cosmogenic ^{3}He in alluvial metal and alloy grains: assessing the potential for quantifying sediment transport times. Chem. Geol. 517, 22–33.
Yin, R., Krabbenhoft, D.P., Bergquist, B.A., Wang, Z., Lepak, R.F., Hurley, J.P., 2016. Effects of mercury and thallium concentrations on high precision determination of mercury isotope composition by Neptune Plus multiple collector inductively coupled plasma mass spectrometry. J. Anal. At. Spectrom. 31, 2060–2068.
Yin, R., Deng, C., Lehmann, B., Sun, G., Lepak, R.F., Hurley, J.P., Zhao, C., Xu, G., Tan, Q., Xie, Z., Hu, R., 2019. Magmatic-hydrothermal origin of mercury in Carlin-style and epithermal gold deposits in China: evidence from mercury stable isotopes. ACS Earth Space Chem. 3, 1631–1639.
Zheng, W., Hintelmann, H., 2010. Nuclear field shift effect in isotope fractionation of mercury during abiotic reduction in the absence of light. J. Phys. Chem. A 114, 4238–4245.